Biochimica et Biophysica Acta 1838 (2014) 1096–1103

Contents lists available at ScienceDirect

Biochimica et Biophysica Acta

journal homepage: www.elsevier.com/locate/bbamem

Viral potassium channels as a robust model system for studies of membrane–protein interaction☆,☆☆

Christian J. Braun [a], Christine Lachnit [a], Patrick Becker [a], Leonhard M. Henkes [b], Cristina Arrigoni [c], Stefan M. Kast [b], Anna Moroni [c,d], Gerhard Thiel [a], Indra Schroeder [a,*]

[a] Membrane Biophysics, Technical University of Darmstadt, Schnittspahnstrasse 3, 64287 Darmstadt, Germany
[b] Physikalische Chemie III, Technische Universität Dortmund, Otto-Hahn-Str. 6, 44227 Dortmund, Germany
[c] Department of Biosciences, University of Milan, Via Celoria 26, 20133 Milano, Italy
[d] CNR-IBF, Via Celoria 26, 20133 Milano, Italy

ARTICLE INFO

Article history:
Received 25 April 2013
Received in revised form 31 May 2013
Accepted 8 June 2013
Available online 17 June 2013

Keywords:
Black lipid membrane
Cell-free protein expression
Membrane–protein interaction
Planar patch clamp
Single-channel measurement
Viral potassium channel

ABSTRACT

The viral channel Kcv_{NTS} belongs to the smallest K^+ channels known so far. A monomer of a functional homotetramer contains only 82 amino acids. As a consequence of the small size the protein is almost fully submerged into the membrane. This suggests that the channel is presumably sensitive to its lipid environment. Here we perform a comparative analysis for the function of the channel protein embedded in three different membrane environments. 1. Single-channel currents of Kcv_{NTS} were recorded with the patch clamp method on the plasma membrane of HEK293 cells. 2. They were also measured after reconstitution of recombinant channel protein into classical planar lipid bilayers and 3. into horizontal bilayers derived from giant unilamellar vesicles (GUVs). The recombinant channel protein was either expressed and purified from *Pichia pastoris* or from a cell-free expression system; for the latter a new approach with nanolipoprotein particles was used. The data show that single-channel activity can be recorded under all experimental conditions. The main functional features of the channel like a large single-channel conductance (80 pS), high open-probability (>50%) and the approximate duration of open and closed dwell times are maintained in all experimental systems. An apparent difference between the approaches was only observed with respect to the unitary conductance, which was ca. 35% lower in HEK293 cells than in the other systems. The reason for this might be explained by the fact that the channel is tagged by GFP when expressed in HEK293 cells. Collectively the data demonstrate that the small viral channel exhibits a robust function in different experimental systems. This justifies an extrapolation of functional data from these systems to the potential performance of the channel in the virus/host interaction. This article is part of a Special Issue entitled: Viral Membrane Proteins—Channels for Cellular Networking.

1. Introduction

Potassium channels are membrane proteins, which catalyze the flux of K^+ ions in a selective and regulated (gated) manner across membranes. Because of their high transport capacity, the activity of single K^+ channels can be measured at high temporal resolution with various electrophysiological methods. This detailed functional information is paralleled by explicit knowledge on the molecular architecture of K^+ channels, which is available from crystal structures [1–3] and MD simulations [4,5]. The combination of these high-resolution data is now frequently used to correlate structural properties with functional features [6,7].

In this context, however, it occurs that for a full understanding of ion channel function the membrane, in which the protein is embedded, has to be considered also. Crystal structures for example reveal the binding of anionic phospholipids to specific pockets in the KcsA protein [8]. Complementary functional studies underscore the role of these interactions for channel function [9–11]. Structural data furthermore suggest that the architecture and orientation of transmembrane domains of membrane proteins are designed in such a way that they avoid a thermodynamically unfavorable hydrophobic mismatch between protein and lipid bilayer [12–14]. This predicts that the thickness of the membrane, which can vary in the plasma membrane within microscopic domains [15], may affect the structure of a channel and as a consequence also its activity. Functional studies in this context have indeed shown that the conductance of the BK channel is depending on the thickness of the lipid bilayer in which it is inserted [16]. But the

Abbreviations: BLM, black lipid membrane; DPhPC, 1,2-diphytanoyl-*sn*-glycero-3-phosphocholine; GUV, giant unilamellar vesicle

☆ This article is part of a Special Issue entitled: Viral Membrane Proteins—Channels for Cellular Networking.

☆☆ Funding support: The investigations were supported by Cariplo grant 2009-3519 (AM, IS), PRIN 2010CSJX4F (AM), Deutsche Forschungsgemeinschaft and by Loewe Cluster Soft-Control (GT, IS).

* Corresponding author. Tel.: +49 6151 16 3503.
E-mail address: schroeder@bio.tu-darmstadt.de (I. Schroeder).

0005-2736/$ – see front matter © 2013 Elsevier B.V. All rights reserved.
http://dx.doi.org/10.1016/j.bbamem.2013.06.010

membrane-spanning domains of the proteins seem to be not the only ones involved in lipid-channel interaction. A recent study suggests that the M0 helix of KcsA, which is lying on the cytosolic membrane interface, performs a "barrel roll" movement upon channel opening; this event seems to be dependent on the presence of anionic lipids in the inner membrane leaflet [17].

The activity of ion channels is generally recorded with the patch clamp method [18] in membranes from living cells, which express a channel of interest in a homologous or heterologous manner. In this case, the composition of the membrane in which the channel functions, is largely unknown and not under the control of the experimenter. In such a system, there is also little control over the arrangement of the channel proteins in clusters, their interaction with endogenous proteins or their insertion into micro-domains like lipid rafts. A reduced system, which offers more control over the environment of a channel protein, is provided by the planar lipid bilayer technique [19,20]. With this method, the lipid bilayer can be chosen and modified by the experimenter on demand. This offers the opportunity to reconstitute a purified protein into a pure and defined bilayer. The problem with this approach is that bilayers may under certain circumstances also generate lipid pores [21] so that bilayer recordings with reconstituted proteins are sometimes challenged as artifacts [22]. Another source of artifacts in bilayer recordings is related to the isolation procedure of the channel proteins. Protein produced recombinantly or isolated from cells may be contaminated with endogenous channel proteins from the expression system [23,24]. A further disadvantage of the bilayer technique is that some protocols require a solvent like decane for building the bilayer [20]. In the procedure some solvent may stay in the bilayer and modify the membrane in an unpredictable fashion. Another technique generates planar lipid bilayers from giant unilamellar vesicles (GUVs) [25]. This approach does not require any solvents; but in this protocol, usually 10% cholesterol is used for the fabrication of stable membranes.

In this work, we compare the basic single-channel properties of a model K^+ channel in a variety of different recording systems. The small viral K^+ channel Kcv_{NTS} is encoded by a *Chlorella* virus isolated from an alkaline lake in Nebraska [26]. Kcv_{NTS} is structurally very similar to Kcv_{ATCV-1} from *Acanthocystis turfacea Chlorella* virus-1 (Fig. 1). The latter is the prototype of the most recently isolated *Chlorella* virus group, which infects SAG type *chlorella* cells [27]. Previous studies have already shown that both viral proteins are functional K^+ channels [26,28]. The interesting aspect in the context of the present work is that Kcv_{ATCV-1} and its orthologs are miniature indeed [29]. The four monomers, which form the functional tetramer, each contain only 82 amino acids. As we will demonstrate below by molecular dynamics (MD) simulations this small channel is quasi fully immersed in the lipid bilayer. We consider this an ideal model system for studying the relevance of protein/bilayer interactions. The environment of the protein is dominated by the lipid bilayer; extracellular or cytosolic domains can, if any, only play a minor role for channel function.

The systematic examination of viral K^+ channel function in different experimental conditions is important for a proper understanding of their role in the virus/host system. The current knowledge is that the great majority of *chlorella* viruses (39 over 41), which were sequenced so far, contain genes for small K^+ channels [30]. Expression studies show that the channel protein is produced as a late gene in the infected host cell [31]. Recent experiments confirm with the help of a monoclonal antibody that the prototype channel Kcv from virus PBCV-1 is indeed present in the mature virion; it is presumably located in the inner membrane of the virus particle [32]. A bulk of circumstantial data suggests that the viral channel has a crucial role during early infection. Measurements of the membrane potential in the host *Chlorella* NC64A, a unicellular green alga, have shown that the cells depolarize within the first few minutes of virus infection [33]. This depolarization is most likely caused by an insertion of few individual viral K^+ channels into the plasma membrane of the host during fusion of virus and host cell membrane [34]. Experimental support for this hypothesis comes from the observation that the same blockers, which inhibit the viral channel in heterologous systems or after reconstitution in planar lipid bilayers, also block the host depolarization [33,34]. The crucial role of the viral channel in host infection is further underscored by experiments, which show that the sensitivity of host depolarization to channel blockers reflects the distinct inhibitor sensitivity of K^+ channel orthologs from different viruses [33]. It was further found that a block of viral K^+ channel activity and the consequent inhibition of the host depolarization prevent infection. The latter could be attributed to a block of DNA ejection from the virus particle into the host [34]. A plausible explanation for this scenario is that the depolarization of the host cell, which is initiated by the viral channel, causes an efflux of K^+ salts and consequently water from the host cells [35]. This lowers the high internal pressure of the host cell and makes it easier for the virus to transfer its large dsDNA genome into the host. This interpretation of viral channel function during infection is based on extrapolations of functional data from heterologous expression systems and from reconstituting the viral channel protein in planar lipid bilayers. Because of the small size of the channels and the aforementioned potential dependency of channel function on the lipid bilayer it was so far not known whether these extrapolations are indeed valid.

The present data now show that conductance and gating properties of the channel are robust and observable in conventional patch clamp recordings and in different planar lipid bilayer experiments. With the exception of a smaller conductance and a slightly lower open-probability in the mammalian cell system, the basic functional features of the channel are maintained in all experimental approaches. There is little difference on whether the protein is synthesized by a mammalian cell, expressed and purified from yeast or produced in a cell-free system. The results of these experiments stress that functional data from different approaches can be used to draw conclusions on structure/function correlates in this miniature channel; the experimental data are also sufficiently general and allow an extrapolation of channel function in the virus/host system.

Fig. 1. Amino acid sequence alignment of Kcv_{ATCV-1} and Kcv_{NTS}. Exchanges are marked in gray, the signature potassium filter sequence is underlined. The predicted location of the two transmembrane helices TM1 and TM2 of Kcv_{ATCV-1} was taken from [28].

2. Methods

2.1. Protein expression in Pichia pastoris

The ORF encoding the Kcv_{NTS} gene was subcloned into a modified *P. pastoris* expression vector pPICZ A (Invitrogen) containing a Kozak consensus sequence, a His7 tag, a proteolytic site for the H3C protease and a LIC (ligation independent cloning) site on the N-terminus of the protein sequence. *P. pastoris* cells (SMD 1163 strain) were transformed with 3 μg of the PmeI linearized construct by using the *Pichia* Easy Comp™ kit as described by the manufacturer (Invitrogen, Carlsbad, CA, USA). Positive colonies were selected from YPDS (10 g/l bacto yeast, 20 g/l bacto peptone and 20 g/l dextrose) agar plates containing 50 μg/ml zeocin. Single-colony starting cultures were grown in BMGYH medium [see the *Pichia* expression kit manual (Invitrogen)] at 30 °C, 300 rpm for 36 h. After centrifugation at 3000 *g* for 10 min at 4 °C, the pellet was resuspended to a D600 of 4 in BMMH medium [see the *Pichia* expression kit manual (Invitrogen)] and grown at 30 °C, 300 rpm for 24 h. Each gram of cells was suspended in a 1:20 ratio of breaking buffer as in Gazzarrini et al. [28]. The presence of the overexpressed protein at the correct molecular weight was verified on SDS-PAGE and Western blot. Cells were broken with a Cell Disruptor (TS Series

Benchtop, Constant System, Inc.) set on a 40 kPa pressure. The cell homogenate was centrifuged at 3000 *g* for 10 min at 4 °C. The supernatant was centrifuged at 30,000 *g* for 45 min at 4 °C in the presence of PEG 8000 10% (w/v) and NaCl 200 mM. The pellet, consisting of the microsomal fraction of the membrane, was solubilized with 200 mM octyl-glucopyranoside (Anatrace) for 4 h at 4 °C. Elution of the protein was performed as in Pagliuca et al. [36], in the presence of 40 mM octyl-glucopyranoside. The integrity and purity of the protein was checked on SDS-PAGE.

2.2. Cell-free protein production and purification

Cell-free production of the Kcv_{NTS} protein was done with the MembraneMax™ *HN* Protein Expression Kit (Invitrogen) following the manufacturer's instructions. The gene of Kcv_{NTS} was cloned into a pEXP5-CT/TOPO®-vector. To express the protein in its native form, a stop-codon was inserted right before the gene of a 6xHis-tag. Briefly, the DNA template was incubated with the synthesis reaction mix (MembraneMax™ *HN* reagent carrying a polyHis-tag, ribosomes, T7 RNA polymerase and energy renewal system) for 35 min at 37 °C (1000 rpm). The feeding buffer was added and the reaction was incubated for 1 h 45 min at 37 °C (1000 rpm). After the expression, the protein was loaded on a Ni–NTA column, which was equilibrated with an equilibration buffer [500 mM NaCl, 30 mM HEPES, 10% glycerin (all from AppliChem GmbH, Darmstadt, Germany), pH 7.5]. Unspecific binding was removed by washing the column with 20 mM imidazole (Sigma Chemical, Deisendorf, Germany) twice. The protein was then eluted with 250 mM imidazole in 7 fractions at 100 μl. After elution the protein was used directly in the planar bilayer system.

2.3. Vertical black lipid membrane (BLM) experiments

Planar lipid bilayers were formed in a vertical bilayer set up (IonoVation, Osnabrück Germany) by the monolayer folding technique [19] over a hole (ca. 100 μm in diameter) in a Teflon foil. The hole was pretreated with a 1% hexadecane solution (MERCK KGaA, Darmstadt, Germany) in n-Hexan (Carl ROTH, Karlsruhe, Germany). In the next step a lipid solution of 1,2-diphytanoyl-*sn*-glycero-3-phosphocholine (DPhPC, 15 mg/ml, from Avanti Polar Lipids, Alabaster, AL, USA) in n-Pentan (MERCK) was pipetted onto the experimental solution (100 mM KCl, 10 mM HEPES, adjusted with KOH to a pH of 7.0). After evaporation of the detergent, the solutions in both chambers were raised to form a lipid bilayer. After formation of the bilayer a voltage protocol was applied for at least 5–10 min to exclude contaminations or unspecific channel activity of e.g. lipid pores [21]. For incorporation of ion channels either in detergent (octyl-glucopyranoside) or imidazole (250 mM) a small amount (1–3 μl) was added into the *trans* compartment directly. After fusion of ion channels with the lipid bilayer different voltage protocols were applied to record the resulting currents.

All planar lipid bilayer measurements were done at room temperature (20–25 °C). Ag/AgCl electrodes were connected to the head-stage of a patch clamp amplifier (L/M-EPC 7, List-Medical, Darmstadt). Membrane potentials are referred to the *cis* compartment. Single-channel currents were filtered at 1 kHz and digitized with a sampling interval of 280 μs (3.57 kHz) by an A/D-converter (LIH 1600, HEKA Electronik, Lambrecht, Germany).

2.4. Preparation of liposomes and formation of horizontal lipid bilayers

Giant unilamellar vesicles (GUVs) were formed by electroformation [37] with the Vesicle Prep Pro station (Nanion Technologies GmbH, München, Germany). The lipid solution contained 10 mM DPhPC and 1 mM synthetic cholesterol (AppliChem), dissolved in chloroform (AppliChem). The preparation of GUVs is reported elsewhere [25]. After formation of GUVs they were used (3 μl) in the Port-a-Patch system (Nanion) directly. GUVs touching the surface of the glass chip burst immediately to form stable lipid bilayers with high ohmic resistance [25]. In case of unstable bilayers a 0.1 M HCl solution was used to stabilize the membrane. After stabilization the HCl solution was washed out with the experimental solution (100 mM KCl, 10 mM HEPES, adjusted with KOH to a pH of 7.0).

To avoid artifacts in the measurements the bilayers were tested prior to the addition of protein for at least 5–10 min; only bilayers which revealed no current fluctuations during the test were used for further experiments. Afterwards, 0.5–2 μl of the protein (solubilized in octyl-glucopyranoside) was added directly onto the chip. After fusion of ion channels with the lipid bilayer different voltage protocols were applied to record the resulting currents. Single-channel currents were filtered at 3 kHz and with a sampling interval of 100 μs (10 kHz) with an EPC9 (HEKA) amplifier.

2.5. HEK cell experiments

Kcv_{NTS} was cloned between the *BglII* and *EcoRI* restriction sites of the multiple cloning site of the pEGPF-N2 vector (BD Biosciences, Heidelberg, Germany). No stop codon was inserted, so EGPF was fused in frame directly to the C-terminus of the channel protein. HEK293 cells were transiently transfected with GeneJuice (MERCK) following the manufacturer's instructions. The experiments were done 24–36 h after transfection; the GFP fluorescence served to identify successfully transfected cells.

Patch clamp recordings were performed in cell-attached and inside-out mode. Pipette and bath solution were identical and contained 100 mM KCl, 1 mM $MgCl_2$, 1.8 mM $CaCl_2$, 10 mM HEPES, and 100 mM mannitol. pH was adjusted to 7.4 with KOH. Pipettes were pulled from borosilicate glass (Science Products, Hofheim, Germany) on a two-step puller (L/M-3P-A, List-Medical) and typically had a resistance of 15–20 MOhm. Currents were measured by a Dagan 3900 amplifier (Dagan Corporation, Minneapolis, MN, USA) and digitized by a LIH 8 + 8 (InstruTECH/HEKA) at a rate of 200 kHz. The low-pass filter on the amplifier was set to 10 kHz or 5 kHz.

2.6. Data analysis

Current traces at different membrane voltages were recorded via Patchmaster (HEKA) and analyzed with Fitmaster (HEKA) and lab-built software (KielPatch, www.zbm.uni-kiel.de/aghansen/software.html). Current amplitudes were determined visually, an automated jump detector [38] was used to construct the open-probability and dwell time histograms. The dwell time histograms were fitted with sums of 1–3 exponential functions.

3. Results and discussion

3.1. Structural properties of Kcv_{NTS}

The Kcv_{NTS} channel is a very close relative of the previously characterized viral channel Kcv_{ATCV-1} [28]; with only 82 amino acids they are the so far smallest known K^+ channels. The alignment shows that both channels differ in only 4 out of 82 amino acids (Fig. 1). When transfected into HEK293 cells Kcv_{NTS} generates macroscopic currents [26], which are similar to those obtained with Kcv_{ATCV-1} [28].

3.2. Comparison of channel activity in different systems

The influence of different systems for channel expression and reconstitution was studied by recording single-channel currents from Kcv_{NTS} under four different experimental conditions:

1.) The channel was produced in *P. pastoris* and the isolated protein reconstituted in a classical planar lipid bilayer (black lipid membranes, BLM).

2.) The channel was produced in a cell-free system and examined in the BLM.
3.) Giant unilamellar vesicles (GUVs) were used to form a horizontal membrane in an integrated planar patch clamp system. Protein from *P. pastoris* was reconstituted into this membrane.
4.) HEK293 cells were transfected with a plasmid containing the gene for a Kcv_{NTS}-GFP fusion protein and examined in a classical patch clamp setup.

Under all experimental conditions, it was possible to measure the single-channel characteristics of Kcv_{NTS}. After achieving in each system the appropriate conditions for single-channel recordings a transmembrane potential was applied. Because of the high open-probability of Kcv_{NTS} (see Fig. 4B, below), the number of active channels could be easily estimated from a simple visual inspection of the current records. Bilayers or patches with no or too many (5 or more) channels were discarded. If current fluctuations of one to four channels were visible, a voltage protocol ranging from −120 to +120 mV with steps of 20 mV was applied. If the membrane stability allowed it, the protocol was repeated multiple times. For the determination of single-channel I/V curves (current voltage relationships) and for the estimation of the open-probability, single- and multi-channel data were used. Dwell-time histograms were obtained from recordings with one channel only.

Fig. 2 shows representative current traces of single Kcv_{NTS} channels at +60 and −60 mV for all four experimental approaches. The characteristics of the channels are consistent under all conditions: the unitary conductance is similar and the channel exhibits very high open-probability throughout. The temporal behavior shows bursts of activity interrupted by short sojourns in a closed state. During bursts of activity, the channel approaches an open-probability of virtually 100% even though it is interrupted by very short closing events. They are visible as incomplete transitions towards the baseline because of the limited temporal

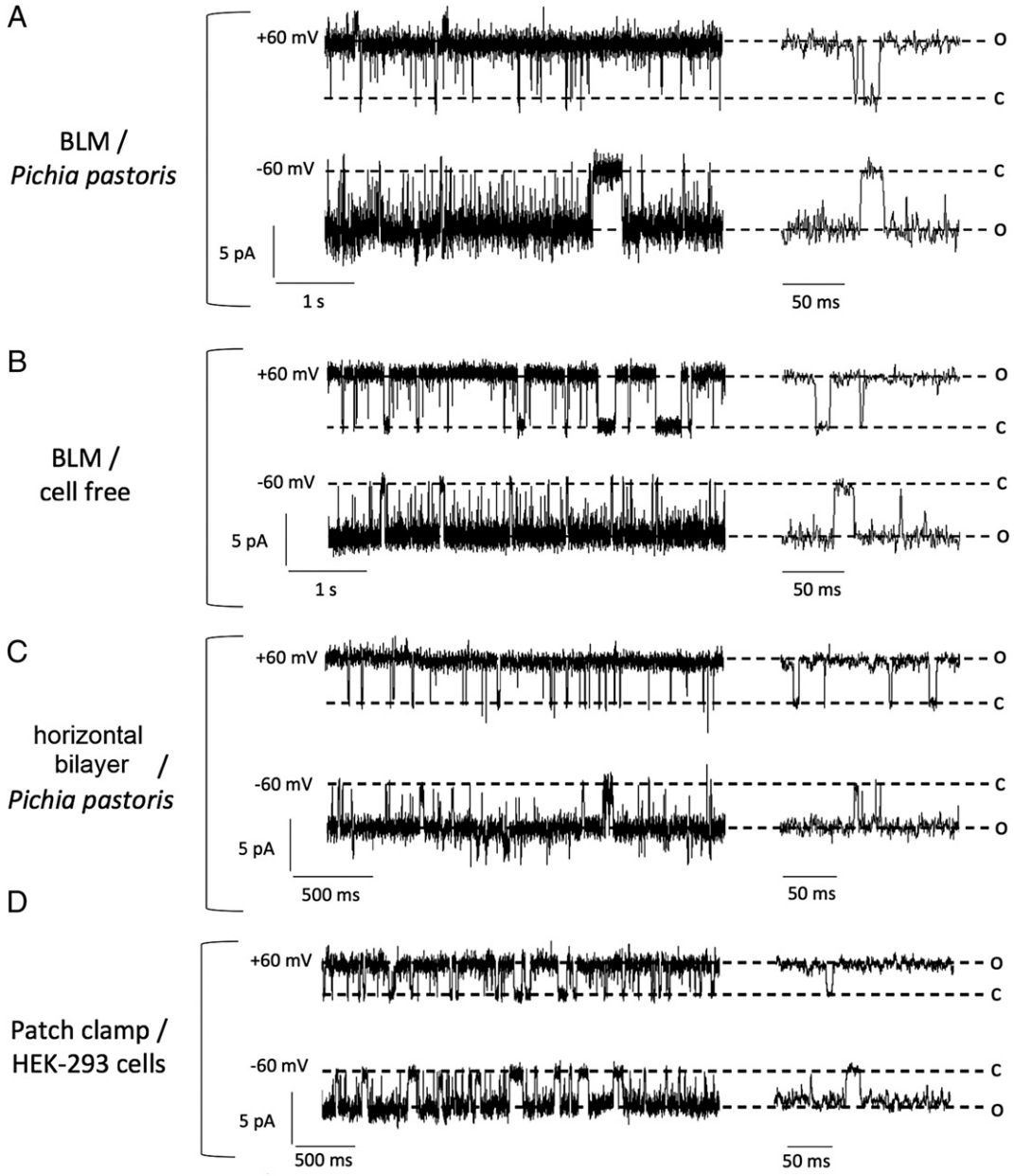

Fig. 2. Representative current traces of single Kcv_{NTS} channels in different expression systems. Currents were recorded in steady state at membrane potentials of +60 mV and −60 mV, respectively. C and O denote the closed and open channel, respectively. (A) Protein produced in *Pichia pastoris* and reconstituted in symmetric planar lipid bilayer. (B) Protein produced in a cell-free system in the same type of bilayer. (C) Protein from *P. pastoris* reconstituted into horizontal membranes formed from GUVs with planar patch clamp. (D) Inside-out patch clamp on HEK293 cells transiently transfected with a Kcv_{NTS}-GFP fusion protein. Data was offline filtered at 500 Hz (A, B) or 1 kHz (C, D).

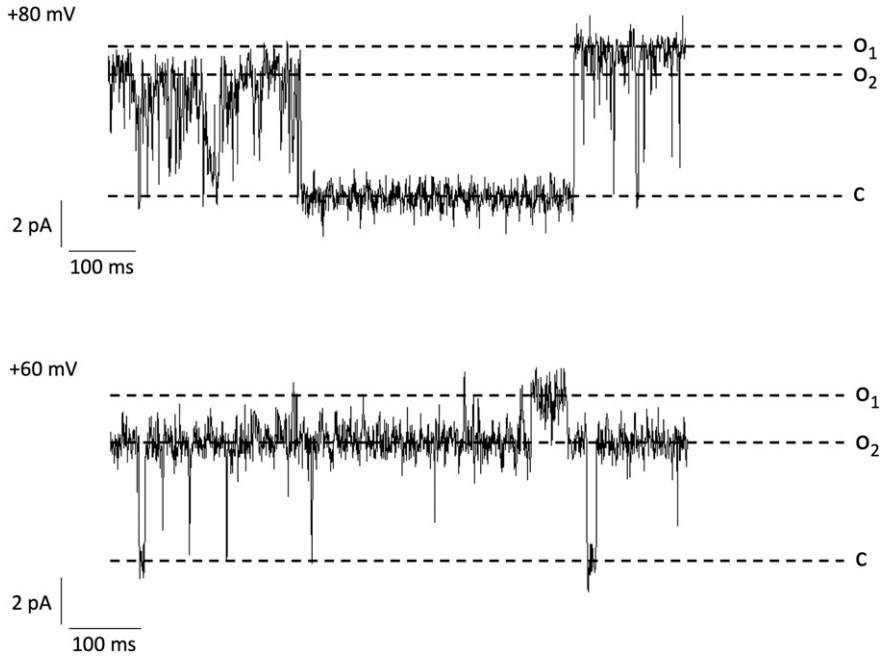

Fig. 3. Subconductance states of a single Kcv_{NTS} channel purified from *Pichia pastoris* and reconstituted in BLM. The dominant current level is O_2. Jumps into a higher level O_1 occur either via a closed state (upper panel) or directly (lower panel).

resolution. The results of these experiments show that the large unitary conductance and the gating with a high open-probability, which is recorded by patch clamp measurements in living cells, are also maintained in the reduced bilayer systems. This overall similarity confirms that the channel fluctuations measured in the bilayer systems are not caused by lipid pores or detergent-induced membrane defects [21]. Also a contamination from the expression system can be excluded as the source of channel activity.

In addition to the prevailing conductance (marked by dashed lines in Fig. 2), the channel occasionally displays other conductance states. This behavior is most obvious in the BLM system, where the channel could fluctuate between the dominant conductance and a level, which exceeded the latter by approximately 30%. The channel is able to switch between the two conductance levels either via a closed state (Fig. 3, upper panel) or directly (lower panel). This indicates that both conductances are indeed a property of Kcv_{NTS} and not introduced by a

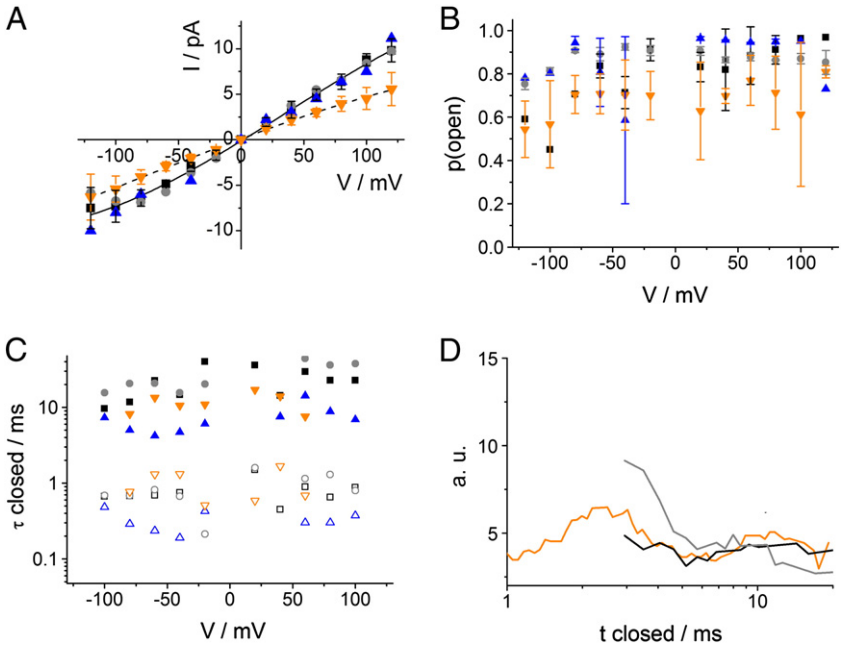

Fig. 4. Electrophysiological properties of Kcv_{NTS} under different experimental conditions. All panels use the same colors and symbols. Black (squares) and gray (circles): reconstitution in BLM with protein from *Pichia pastoris* and from cell-free synthesis, respectively. Blue (upright triangles): horizontal bilayers formed from GUVs by planar patch clamp. Orange (inverted triangles): patch clamp recordings on HEK cells. (A) Single-channel I/V curves of the dominant conductivity. Number of experiments: *P. pastoris* (n = 5) and cell-free production in BLM (n = 4), *Pichia* protein in horizontal bilayers (n = 2) and transfected HEK cells (n = 9, cell-attached and inside-out data were pooled). For clarity, the standard deviation is only shown for the HEK cell experiments and the *Pichia* protein in BLM. The lines are polynomial fits (without theoretical meaning) to the HEK cell data (dashed) and the other three conditions (solid line). (B) Single-channel open-probability. (C) Time constants of closed dwell times from one representative experiment for each condition. Open and closed symbols denote the two different time constants. (D) Representative closed dwell time histograms obtained at −60 mV from BLM and HEK cells.

Table 1
Single-channel conductivity of Kcv_{NTS} in 100 mM KCl in different systems as determined by a linear fit from −60 to +60 mV to the I/V curves from several experiments. The number of experiments is given in brackets. From the channel protein expressed in *P. pastoris* and reconstituted in the planar patch clamp set up, only two data sets are available. The individual conductance values, which are appreciably different, are given instead of the average.

Pichia/BLM	81 ± 7 pS (5)
In vitro/BLM	87 ± 6 pS (4)
Pichia/planar patch clamp	68/80 pS (2)
HEK	50 ± 6 pS (9)

contamination. Because these types of fluctuations between a sub-state and a fully open state were not observed in all measurements it is possible that the unitary conductance of the channel is underestimated in the data of the I/V relation.

The single-channel I/V curve of the dominant conductance level is essentially linear over the voltage range tested (Fig. 4A). The slope conductance between +60 mV and −60 mV lies between 50 and 90 pS for the different recording conditions. The results are summarized in Table 1. There was no apparent difference between the unitary conductance measured in cell-attached and inside-out experiments on HEK293 cells; the data were therefore pooled for the I/V relation. A comparison of the unitary conductance values from different methods shows that the conductivity of the channel in HEK293 cells was significantly lower (50 pS) than in the artificial systems (~80 pS). The present data cannot answer the question of why the unitary conductance is lower in cells than in the bilayers systems. The similarity in channel conductance from records in cell-attached mode and excised patches excludes cytosolic factors as an explanation for the low conductance in cells. One reason could be that the channel, which is expressed in HEK293 cells is C-terminally tagged with GFP. This explanation is plausible because the single-channel conductance of the similar Kcv_{ATCV-1} channel (Fig. 1) is also 80 pS when measured without a GFP tag in the plasma membrane of *Xenopus* oocytes [28]. This value corresponds to the conductance of Kcv_{NTS} in artificial bilayers (Table 1). In patch clamp experiments in HEK cells, GFP-tagged Kcv_{ATCV-1} also shows a lower conductance (data not shown). The results of these experiments suggest that the unitary conductance of the channel is not per se smaller in a native plasma membrane.

We quantified the gating of the channel by calculating the open-probabilities and, where possible, time constants from dwell-time histograms. Fig. 4B shows that the open-probability is practically voltage-independent and similar under all experimental conditions tested. The open-probability has an average of about 80%. Such a high open-probability has already been found for the close relative of Kcv_{NTS}: Kcv_{ATCV-1} also has a single-channel open-probability of about 80% in *Xenopus* oocytes [28] as well as in HEK293 cells (data not shown).

Dwell-time histograms were constructed and exponential fits of the closed-state histograms revealed two different time constants (Fig. 4C) in all four systems. A third, faster, time constant could be observed only in HEK cells (not shown), most likely because of the faster filtering and sampling in the patch clamp setup compared to the artificial bilayers. As expected from the overall open-probability, the time constants do not depend appreciably on the membrane potential; they are also within the scatter independent of the expression and recording system.

3.3. The small Kcv_{NTS} like channels are fully embedded in the lipid bilayer

The data show that the small Kcv_{NTS} channel maintains its overall activity in a variety of experimental systems. It will be a future goal to understand the correlations between structure of a channel in its membrane environment and function in more detail. To tackle this problem we illustrate the membrane location of such a short channel by performing preliminary MD simulations of the Kcv_{ATCV-1} variant. Omitting details of the model building process, which follows closely

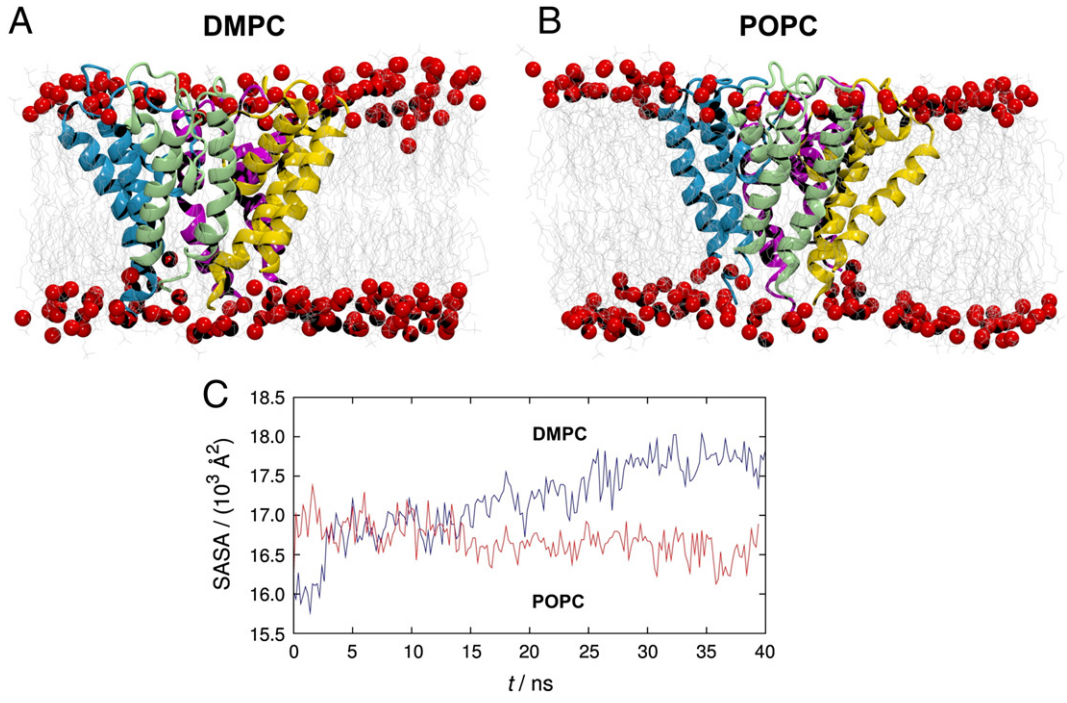

Fig. 5. Results of MD simulations of Kcv_{ATCV-1} in DMPC and POPC membranes. Two snapshot structures after a total simulation time of 40 ns are shown for DMPC (A) and POPC (B) embedding. The channel monomers are depicted in cartoon representation and are colored individually. Lipid headgroups are shown as red balls, hydrocarbon tails as wire. Solvent components have been omitted for clarity. (C) The solvent-accessible surface area (SASA) is shown as a function of simulation time (blue: DMPC, red: POPC), indicating different overall shape in response to varying membrane environments. All calculations and visualizations have been done using VMD [41].

our earlier simulation studies of truncated KirBac1.1 [4] and Kcv_{PBCV-1} [39] in a solvated DMPC membrane and which will be described elsewhere, a homology model was derived from the X-ray crystallographic KirBac1.1 structure [40], embedded in two different membrane environments, DMPC (fully saturated) and POPC (unsaturated), built-up using VMD 1.9 [41] by cutting overlapping lipid molecules from an initial 256 lipid bilayer, and simulated with NAMD 2.9 [42] in 0.1 M aqueous KCl solution at 310 K and 1 bar with a time step of 2 fs on the basis of the CHARMM22 force field [43,44].

The key result is that this very short channel is practically fully immersed in the relatively thin lipid bilayers. This is illustrated in Fig. 5, which shows snapshot structures in DMPC and POPC after 40 ns simulation time. The protein remains very stable over several tens of nanoseconds although the different membrane environments induce structural modulations, which will be further analyzed in future work. As a signature, we show the diverging trends of the solvent-accessible surface of the two simulation setups, which indicate slightly differing overall shapes of the protein (Fig. 5C).

4. Conclusion

The comparative analysis of Kcv_{NTS} activity shows that the channel maintains its basic functional features under all four experimental conditions. There is no appreciable difference between recordings in a classical bilayer system, which still contains some solvent, and the solvent free bilayer. The absence of a solvent effect is consistent with previous data, which also found no difference on channel function between bilayers with or without solvent [20]. The present data also show no systematic difference between the function of channel proteins obtained from a cell-free expression system or from expression in *P. pastoris*. The results of these experiments suggest that the protein is properly folded after the different purification procedures. It also occurs that the scaffold protein, which surrounds the channel in the cell-free expression system [45], is not affecting channel fold or function. The technique of inserting membrane proteins into nanoscale membrane disks held together by scaffold proteins has been already successfully used for pharmacological [46] and NMR studies [47]. To our knowledge, we present here the first case of an electrophysiological application of this system.

The robust function of the channel in different membrane environments and the prevailing high single-channel open-probability of $P > 0.5$ in all experimental conditions support the notion that gating is not dramatically affected by the experimental conditions tested here. The results of these experiments are important for a further understanding of the role of the viral channel in infection of the host cell. It appears that data on channel conductance and activity obtained from heterologous expression in cells or from reconstitution of the channel in bilayers can be directly extrapolated into the situation in the host cell.

The present data from the functional assays are also interesting in the context of the computational data. The MD simulations of the small Kcv_{ATCV-1} channel in different membranes imply that the microscopic structure of the channel can be influenced by the thickness of the bilayer. If these structural changes, which are imposed by the membrane, turn out to be functionally relevant we can assume that a DPhPC membrane, which is used in the bilayer methods, is sufficiently mimicking the plasma membrane of a mammalian cell.

Acknowledgements

We thank J. Van Etten (Lincoln, USA) and T. Greiner (Darmstadt) for initial characterization of the Kcv_{NTS} channel and also U.P. Hansen (Kiel) for suggestions to the manuscript.

LMH and SMK thank the IT & Media Center of the TU Dortmund for providing computer time on the LiDOng cluster.

References

[1] D.A. Doyle, The structure of the potassium channel: molecular basis of K^+ conduction and selectivity, Science 280 (1998) 69–77.
[2] D.A. Doyle, Structural changes during ion channel gating, Trends Neurosci. 27 (2004) 298–302.
[3] J.S. Santos, G.A. Asmar-Rovira, G.W. Han, W. Liu, R. Syeda, V. Cherezov, K.A. Baker, R.C. Stevens, M. Montal, Crystal structure of a voltage-gated K channel pore module in a closed state in lipid membranes, J. Biol. Chem. 287 (2012) 43063–43070.
[4] S. Tayefeh, T. Kloss, G. Thiel, B. Hertel, A. Moroni, S.M. Kast, Molecular dynamics simulation of the cytosolic mouth in Kcv-type potassium channels, Biochemistry 46 (2007) 4826–4839.
[5] W. Treptow, M.L. Klein, Computer simulations of voltage-gated cation channels, J. Phys. Chem. Lett. 3 (2012) 1017–1023.
[6] B. Roux, Ion conduction and selectivity in K^+ channels, Annu. Rev. Biophys. Biomol. Struct. 34 (2005) 153–171.
[7] S.M. Kast, T. Kloss, S. Tayefeh, G. Thiel, A minimalist model for ion partitioning and competition in a K^+ channel selectivity filter, J. Gen. Physiol. 138 (2011) 371–373.
[8] F.I. Valiyaveetil, Y. Zhou, R. MacKinnon, Lipids in the structure, folding, and function of the KcsA K^+ channel, Biochemistry 41 (2002) 10771–10777.
[9] A.M. Dopico, A.N. Bukiya, A.K. Singh, Large conductance, calcium- and voltage-gated potassium (BK) channels: regulation by cholesterol, Pharmacol. Ther. 135 (2012) 133–150.
[10] A.A. Rodriguez-Menchaca, S.K. Adney, Q.-Y. Tang, X.-Y. Meng, A. Rosenhouse-Dantsker, M. Cui, D.E. Logothetis, PIP2 controls voltage-sensor movement and pore opening of Kv channels through the S4–S5 linker, Proc. Natl. Acad. Sci. U. S. A. 109 (2012) E2399–E2408.
[11] H.M. Seeger, L. Aldrovandi, A. Alessandrini, P. Facci, Changes in single K^+ channel behavior induced by a lipid phase transition, Biophys. J. 99 (2010) 3675–3683.
[12] J.A. Killian, Synthetic peptides as models for intrinsic membrane proteins, FEBS Lett. 555 (2003) 134–138.
[13] B. Hertel, S. Tayefeh, M. Mehmel, S.M. Kast, J.L. Van Etten, A. Moroni, G. Thiel, Elongation of outer transmembrane domain alters function of miniature K^+ channel Kcv, J. Membr. Biol. 210 (2006) 21–29.
[14] T. Kim, K. Il Lee, P. Morris, R.W. Pastor, O.S. Andersen, W. Im, Influence of hydrophobic mismatch on structures and dynamics of gramicidin a and lipid bilayers, Biophys. J. 102 (2012) 1551–1560.
[15] K. Simons, J.L. Sampaio, Membrane organization and lipid rafts, Cold Spring Harb. Perspect. Biol. 3 (2011) a004697.
[16] C. Yuan, R.J. O'Connell, P.L. Feinberg-Zadek, L.J. Johnston, S.N. Treistman, Bilayer thickness modulates the conductance of the BK channel in model membranes, Biophys. J. 86 (2004) 3620–3633.
[17] M. Iwamoto, S. Oiki, Amphipathic antenna of an inward rectifier K^+ channel responds to changes in the inner membrane leaflet, Proc. Natl. Acad. Sci. U. S. A. 110 (2012).
[18] E. Neher, B. Sakman, Single-channel currents recorded from membrane of denerved frog muscle fibres, Nature 260 (1976) 799–802.
[19] M. Montal, P. Mueller, Formation of bimolecular membranes from lipid monolayers and a study of their electrical properties, Proc. Natl. Acad. Sci. U. S. A. 69 (1972) 3561–3566.
[20] A.J. Williams, An introduction to the methods available for ion channel reconstitution, in: D. Ogden (Ed.), Microelectrode Techniques: In Plymouth Workshop Handbook, 2nd ed., The company of Biologists, Cambridge, 1994, pp. 79–99.
[21] K.R. Laub, K. Witschas, A. Blicher, S.B. Madsen, A. Lückhoff, T. Heimburg, Comparing ion conductance recordings of synthetic lipid bilayers with cell membranes containing TRP channels, Biochim. Biophys. Acta 1818 (2012) 1123–1134.
[22] L. Becucci, M. Papina, R. Verardi, G. Veglia, R. Guidelli, Phospholamban and its phosphorylated form require non-physiological transmembrane potentials to translate ions, Soft Matter 8 (2012) 3881–3888.
[23] A. Accardi, L. Kolmakova-Partensky, C. Williams, C. Miller, Ionic currents mediated by a prokaryotic homologue of CLC Cl^- channels, J. Gen. Physiol. 123 (2004) 109–119.
[24] P. Labarca, R. Latorre, Insertion of ion channels into planar lipid bilayers by vesicle fusion, Methods Enzymol. 207 (1992).
[25] M. Kreir, C. Farre, M. Beckler, M. George, N. Fertig, Rapid screening of membrane protein activity: electrophysiological analysis of OmpF reconstituted in proteoliposomes, Lab Chip 8 (2008) 587–595.
[26] T. Greiner, Characterization of Novel Potassium Transport Proteins from *Chlorella* Viruses, Technical University of Darmstadt, 2011.
[27] J.A. Bubeck, A.J.P. Pfitzner, Isolation and characterization of a new type of chlorovirus that infects an endosymbiotic *Chlorella* strain of the heliozoon *Acanthocystis turfacea*, J. Gen. Virol. 86 (2005) 2871–2877.
[28] S. Gazzarrini, M. Kang, A. Abenavoli, G. Romani, C. Olivari, D. Gaslini, G. Ferrara, J.L. Van Etten, M. Kreim, S.M. Kast, G. Thiel, A. Moroni, *Chlorella* virus ATCV-1 encodes a functional potassium channel of 82 amino acids, Biochem. J. 420 (2009) 295–303.
[29] G. Thiel, D. Baumeister, I. Schroeder, S.M. Kast, J.L. Van Etten, A. Moroni, Minimal art: or why small viral K^+ channels are good tools for understanding basic structure and function relations, Biochim. Biophys. Acta 1808 (2011) 580–588.
[30] A. Jeanniard, D.D. Dunigan, J.R. Gurnon, I.V. Agarkova, M. Kang, J. Vitek, G. Duncan, O.W. McClung, M. Larsen, J.-M. Claverie, J.L. Van Etten, G. Blanc, Towards defining the chloroviruses: a genomic journey through a genus of large DNA viruses, BMC Genomics 14 (2013) 158.
[31] M. Kang, M. Graves, M. Mehmel, A. Moroni, S. Gazzarrini, G. Thiel, J.R. Gurnon, J.L. Van Etten, Genetic diversity in *chlorella* viruses flanking kcv, a gene that encodes a potassium ion channel protein, Virology 326 (2004) 150–159.
[32] G. Romani, A. Piotrowski, S. Hillmer, S. Gazzarrini, J.R. Gurnon, J.L. Van Etten, A. Moroni, G. Thiel, B. Hertel, Viral encoded potassium ion channel is a structural protein in the chlorovirus PBCV-1 virion, (2013) (unpublished data).

[33] F. Frohns, A. Käsmann, D. Kramer, B. Schäfer, M. Mehmel, M. Kang, J.L. Van Etten, S. Gazzarrini, A. Moroni, G. Thiel, Potassium ion channels of *chlorella* viruses cause rapid depolarization of host cells during infection, J. Virol. 80 (2006) 2437.
[34] G. Thiel, A. Moroni, D.D. Dunigan, J.L. Van Etten, Initial events associated with virus PBCV-1 infection of *Chlorella* NC64A, Prog. Bot. 71 (2010) 169–183.
[35] M. Neupärtl, C. Meyer, I. Woll, F. Frohns, M. Kang, J.L. Van Etten, D. Kramer, B. Hertel, A. Moroni, G. Thiel, *Chlorella* viruses evoke a rapid release of K^+ from host cells during the early phase of infection, Virology 372 (2008) 340–348.
[36] C. Pagliuca, T.A. Goetze, R. Wagner, G. Thiel, A. Moroni, D. Parcej, Molecular properties of Kcv, a virus encoded K^+ channel, Biochemistry 46 (2007) 1079–1090.
[37] P. Walde, K. Cosentino, H. Engel, P. Stano, Giant vesicles: preparations and applications, ChemBioChem 11 (2010) 848–865.
[38] R. Schultze, S. Draber, A nonlinear filter algorithm for the detection of jumps in patch-clamp data, J. Membr. Biol. 132 (1993) 41–52.
[39] S. Tayefeh, T. Kloss, M. Kreim, M. Gebhardt, D. Baumeister, B. Hertel, C. Richter, H. Schwalbe, A. Moroni, G. Thiel, S.M. Kast, Model development for the viral Kcv potassium channel, Biophys. J. 96 (2009) 485–498.
[40] A. Kuo, J.M. Gulbis, J.F. Antcliff, T. Rahman, E.D. Lowe, J. Zimmer, J. Cuthbertson, F.M. Ashcroft, T. Ezaki, D.A. Doyle, Crystal structure of the potassium channel KirBac11 in the closed state, Science 300 (2003) 1922–1926.
[41] W. Humphrey, A. Dahlke, K. Schulten, VMD—visual molecular dynamics, J. Mol. Graphics 14 (1996) 33–38.
[42] J.C. Phillips, R. Braun, W. Wang, J. Gumbart, E. Tajkhorshid, E. Villa, C. Chipot, R.D. Skeel, L. Kalé, Scalable molecular dynamics with NAMD, J. Comput. Chem. 26 (2008) 1781–1802.
[43] M. Schlenkrich, J. Brickmann, A.D.J. MacKerell, M. Karplus, An empirical potential energy function for phospholipids: criteria for parameter optimization and applications, in: K.M. Merz, B. Roux (Eds.), Biological Membranes: A Molecular Perspective from Computation and Experiment, Birkhäuser, Boston, 1996, pp. 31–81.
[44] A.D.J. MacKerell, D. Bashford, M. Bellott, R.L.J. Dunbrack, J.D. Evanseck, M.J. Field, S. Fischer, J. Gao, H. Guo, S. Ha, D. Joseph-McCarthy, L. Kuchnir, K. Kuczera, F.T.K. Lau, C. Mattos, S. Michnick, T. Ngo, D.T. Nguyen, B. Prodhom, W.E.I. Reiher, et al., All-atom empirical potential for molecular modeling and dynamics studies of proteins, J. Phys. Chem. B 5647 (1998) 3586–3616.
[45] F. Katzen, J.E. Fletcher, J.-P. Yang, D. Kang, T.C. Peterson, J.A. Cappuccio, C.D. Blanchette, T. Sulchek, B.A. Chromy, P.D. Hoeprich, M.A. Coleman, W. Kudlicki, Insertion of membrane proteins into discoidal membranes using a cell-free protein expression approach, J. Proteome Res. 7 (2008) 3535–3542.
[46] J.-P. Yang, T. Cirico, F. Katzen, T.C. Peterson, W. Kudlicki, Cell-free synthesis of a functional G protein-coupled receptor complexed with nanometer scale bilayer discs, BMC Biotechnol. 11 (2011) 57.
[47] C. Tzitzilonis, C. Eichmann, I. Maslennikov, S. Choe, R. Riek, Detergent/nanodisc screening for high-resolution NMR studies of an integral membrane protein containing a cytoplasmic domain, PLoS One 8 (2013) e54378.